JOURNAL OF GEOPHYSICAL RESEARCH, VOL. 92, NO. C6, PAGES 6488–6494, JUNE 15, 1987

A Comparison of Methods for Estimating u_* From Given u_z and Air-Sea Temperature Differences

PAUL C. LIU AND DAVID J. SCHWAB

Great Lakes Environmental Research Laboratory, National Oceanic and Atmospheric Administration, Ann Arbor, Michigan

This paper presents an objective assessment of four methods for estimating sea surface friction velocity u_* from wind speed at height z, u_z, and air-sea temperature difference. The methods are compared by using the computed friction velocity as the normalization factor in parametric correlations of wind-wave parameters with the wind and wave measurements made by NOMAD buoys in the Great Lakes. The results show that (1) wind profile parameters obtained from the four methods are generally comparable, (2) parametric correlations with parameters normalized by u_* lead to significantly decreased percentage deviations over correlations normalized by u_z, and (3) correlations based on u_* derived from the four methods show nearly identical percentage deviations. The conclusions are that (1) u_* normalization acts to eliminate the effect of atmospheric stability and (2) any of the four methods can be used effectively in practical applications.

1. INTRODUCTION

One of the basic tools for studying wind waves, surface currents, mixing, and sea-air interactions in the upper ocean is to nondimensionalize the relevant parameters in order to find universal correlations for use with theoretical models. Wind speed at 10 m above sea surface, u_{10}, has frequently been used in the nondimensionalization. While it is convenient to use u_{10}, many routinely available wind speeds are measured at other levels, that is, 19.5 m from a ship or 5 m from a buoy. To reconcile these different wind measurements as well as to eliminate the effects of surface roughness and atmospheric stability, the friction velocity u_* is used for nondimensionalization. As u_* is not a readily measured parameter, a number of empirical methods have been developed to obtain u_* from measurements of u_z and air-sea temperature differences. In this paper we examine four of these methods and apply them to the wind, wave, and temperature data recorded from NOMAD buoys deployed in the Great Lakes. Since in this case there is no measured u_* for direct verification of the results, we simply apply the estimated u_* to correlations of wind-wave parameters. We expect that an effectively estimated u_* will be free from atmospheric stability effects, and hence its application in the parametric wind-wave correlations will act to reduce the scatter.

2. METHODS

The four empirical methods we examine in this paper are (1) the Great Lakes Environmental Research Laboratory (GLERL) method [*Schwab*, 1978] based on the works of *Long and Shaffer* [1975], *Businger et al.* [1971], and *Smith and Banke* [1975], (2) the Kondo method based on *Kondo* [1975], (3) the Large and Pond method based on *Large and Pond* [1981, 1982] and *Keller et al.* [1985], and (4) the Smith method based on *Smith* [1981] and *Dyer* [1975]. All four methods start with the similarity theory of *Monin and Obukhov* [1954] that expresses wind shear and temperature gradient in the form

$$\partial u/\partial z = (u_*/kz)\phi_m(\zeta) \tag{1}$$

$$\partial \theta/\partial z = (\theta_*/kz)\phi_h(\zeta) \tag{2}$$

respectively, where u_* is the friction wind velocity, θ_* is the scaling temperature, $k = 0.4$ is the von Karman constant, $\zeta = z/L$ is the dimensionless stability height, and $L = \theta u_*^2/(gk\theta_*)$ is the Monin-Obukhov stability length.

One difference in the methods tested here is in the definition of functions $\phi_m(\zeta)$ and $\phi_h(\zeta)$ by the authors listed in Table 1. The functions are shown graphically in Figure 1. While the differences are almost nonexistent for unstable cases with $\zeta < 0$, the functions tend to diverge, in some cases significantly, for the stable case with large ζ. Following *Paulson* [1970] we can integrate (1) and (2) to give the wind and temperature profiles as:

$$u = (u_*/k)[\ln (z/z_0) - \psi_m] \tag{3}$$

$$\theta = \theta_0 + (\theta_*/k)[\ln (z/z_0) - \psi_h] \tag{4}$$

where z_0 is the surface roughness length, θ_0 is the extrapolated temperature at $z = 0$, and the expressions of $\psi_m(\zeta)$ and $\psi_h(\zeta)$ corresponding to ϕ_m and ϕ_h are those listed in Table 2. Note in Table 2 that *Long and Shaffer* [1975] further divide the stable condition into two parts: the upper part for mildly stable cases (that is, $0 < \zeta < 1$) and the lower part for strongly stable cases ($\zeta \geq 1$). These solutions are functions of three unknown parameters: u_*, z_0, and L. Different authors have devised their own methods for estimating L. In addition, u_* can be linked with wind speed u_z or z_0 through various theoretical or empirical relations. The *Charnock* [1955] relation, for example, states that gz_0/u_*^2 is a universal constant, where g is the gravitational acceleration; hence z_0, characterizing the aerodynamic roughness at the surface, is proportional to u_*^2. *Smith* [1981] further postulated that roughness length for a smooth surface should be added to achieve gradual transitions from smooth to rough surface conditions. Thus

$$z_0 = au_*^2/g + (\nu/u_*) \exp(-5.5k) \tag{5}$$

where a is the Charnock constant, and ν is the dynamic viscosity of air ($\approx 14 \times 10^{-6}$ m^2 s^{-1}).

This paper is not subject to U.S. copyright. Published in 1987 by the American Geophysical Union.

Paper number 7C0228.

TABLE 1. Wind Shear and Temperature Gradient Functions as Given by Different Authors

	$\phi_m(\zeta)$		$\phi_n(\zeta)$	
	Stable	Unstable	Stable	Unstable
Businger et al. [1971] (GLERL)	$1. + 4.7\zeta$	$(1. - 15.\zeta)^{-1/4}$	$0.74 + 4.7\zeta$	$0.74(1. - 9.\zeta)^{-1/2}$
Kondo [1975])	$1. + 6.\zeta/(1. + \zeta)$	$(1. - 16.\zeta)^{-1/4}$	$1. + 6.\zeta/(1. + \zeta)$	$(1. - 16.\zeta)^{-1/2}$
Large and Pond [1981]	$1. + 7.\zeta$	$(1. - 16.\zeta)^{-1/4}$	$1. + 7.\zeta$	$(1. - 16.\zeta)^{-1/2}$
Dyer [1975], *Smith* [1981]	$1. + 5.\zeta$	$(1. - 16.\zeta)^{-1/4}$	$1. + 5.\zeta$	$(1. - 16.\zeta)^{-1/2}$

In general, all four methods follow a two-stage approach: first, obtain the neutral bulk coefficient and then use air-sea temperature differences to estimate the diabatic conditions. In Smith's method the neutral bulk coefficient is given by

$$C_{zn} = k/\ln (z/z_0)^2 \tag{6}$$

which can be estimated iteratively along with (5). Kondo's method, on the other hand, obtains C_{zn} from the neutral 10-m-level-bulk coefficient by

$$C_{zn} = k^2[kC_{10_n}{}^{-1/2} + \ln (z/10)]^{-2} \tag{7}$$

In the work by *Kondo* [1975], C_{10_n} is empirically related to the wind speed by:

$$\begin{aligned}
10^3C_{10_n} &= 1.08u_{10}{}^{-0.15} && 0 < u_{10} \le 2.2 \text{ ms}^{-1} \\
10^3C_{10_n} &= 0.771 + 0.0858u_{10} && 2.2 < u_{10} \le 5 \text{ ms}^{-1} \\
10^3C_{10_n} &= 0.867 + 0.0667u_{10} && 5 < u_{10} \le 8 \text{ ms}^{-1} \\
10^3C_{10_n} &= 1.2 + 0.025u_{10} && 8 < u_{10} \le 25 \text{ ms}^{-1} \\
10^3C_{10_n} &= 0.773 && 25 < u_{10} < 50 \text{ ms}^{-1}
\end{aligned} \tag{8}$$

Note here that u_{10} is the neutral 10-m-level wind speed. To proceed with a nonneutral u_z, *Kondo* [1975] gave a simple iteration procedure that can be used to obtain an estimate of neutral u_{10}. *Large and Pond*'s [1981] first-stage approach is similar to Kondo's method except that they used a simpler empirical formulation for C_{10_n}:

$$\begin{aligned}
10^3C_{10_n} &= 1.14 && 0 < u_{10} \le 10 \text{ ms}^{-1} \\
10^3C_{10_n} &= 0.49 + 0.065u_{10} && 10 < u_{10} < 50 \text{ ms}^{-1}
\end{aligned} \tag{9}$$

The GLERL approach uses the Charnock relation to obtain z_0 with the Charnock constant determined from setting $u_{10} = 15$ ms^{-1} in the C_{10_n} versus u_{10} relation given by *Smith and Banke* [1975] as:

$$10^3C_{10_n} = 0.63 + 0.066u_{10} \tag{10}$$

In the second stage the GLERL method uses the iteration scheme of *Long and Shaffer* [1975] to obtain L and hence the values of ψ. *Large and Pond* [1981] developed semitheoretical formulas for directly calculating ζ from given wind speed u_z, air temperature T_a, and sea temperature T_s, in which the u_* calculation is given by *Keller et al.* [1985] as:

$$u_* = u_z(C_{zn})^{1/2}/[1 - (C_{zn})^{1/2}\psi_m/k] \tag{11}$$

The *Smith* [1981] approach requires iterations in which u_*, θ_*, and ψ functions are adjusted to yield the desired C_{zn}. *Kondo* [1975] perhaps provided the most simplified approach by developing approximate formulas for calculating C_z from a neutral C_{zn}.

Figure 2 presents plots of C_{10} versus u_{10} for different air-sea temperature differences with the four methods. The neutral stratification case is shown by the heavy line. The thin lines correspond to air-sea temperature differences ranging from -20°C (curves above the neutral curve) to $+20$°C (curves below the neutral curve) at 1°C increments. The main differences are at wind speeds less than 2.5 ms^{-1}; the Kondo, Large-Pond, and Smith methods show the unstable drag coefficient increasing as wind speed decreases to zero, while the GLERL method shows it continuously decreasing. This is clearly a result of the different formulations of the methods.

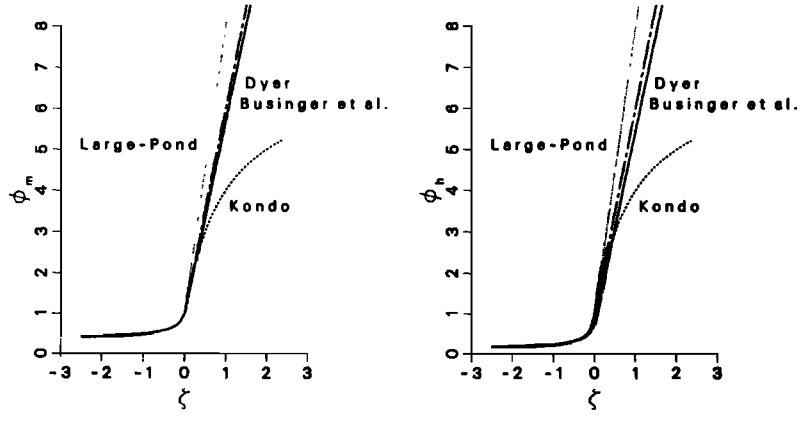

Fig. 1. Comparison of different wind shear and temperature gradient formulas.

TABLE 2. Diabatic Wind and Temperature Profiles as Given by Different Authors

	$\psi_m(\zeta)$	
	Stable	Unstable*
Long and Shaffer [1975] (GLERL)	$0.74 \ln(\zeta/\zeta_0) + 4.7(\zeta - \zeta_0) - \ln\zeta_0 + 4.7/\zeta_0 + 5.7 \ln\zeta$	$\ln[(x-1)(1+x_0)/(1+x)(x_0-1)] + 2[\tan^{-1}x - \tan^{-1}x_0]$
Kondo [1975]	$\ln(\zeta/\zeta_0) + 6 \ln[(1+\zeta)/(1+\zeta_0)]$	$\ln[(x_0^2+1)(x_0+1)^2/(x^2+1)(x+1)^2] + \ln(\zeta/\zeta_0) + 2[\tan^{-1}x - \tan^{-1}x_0]$
Large and Pond [1981]	$-7.\zeta$	$2 \ln[(1+x)/2] + \ln[(1+x^2)/2] - 2\tan^{-1}x + \pi/2$
Smith [1981]	$-5.\zeta$	$2 \ln[(1+x)/2] + \ln[(1+x^2)/2] - 2\tan^{-1}x + \pi/2$
	$\psi_h(\zeta)$	
	Stable	Unstable*
Long and Shaffer [1975] (GLERL)	$\ln(\zeta/\zeta_0) + 4.7(\zeta - \zeta_0) - 0.74\ln\zeta_0 + 4.7/\zeta_0 + 5.44\ln\zeta$	$0.74 \ln[(x^2-1)(x_0^2+1)/(x^2+1)(x_0^2-1)]$
Kondo [1975]	$\ln(\zeta/\zeta_0) + 6 \ln[(1+\zeta)/(1+\zeta_0)]$	$\ln[(x+1)(x_0+1)/(x_0-1)(x+1)]$
Large and Pond [1981]	$-7.\zeta$	$\ln[(1+x^2)/2]$
Smith [1981]	$-5.\zeta$	$2 \ln[(1+x^2)/2]$

*Where $x = (1 - a\zeta)^{1/4}$, $x_0 = (1 - a\zeta_0)^{1/4}$, and $a = 15.$ or 16.

While the methods have different emphases which possibly tend to accentuate each author's own data, the differences are generally no greater than the data point scatter from which they were derived. All four methods can be readily used to estimate a wind profile and hence u_* from a given wind speed and air-sea temperature difference. In the following we shall compare the results as they are applied to actual wind and wave measurements.

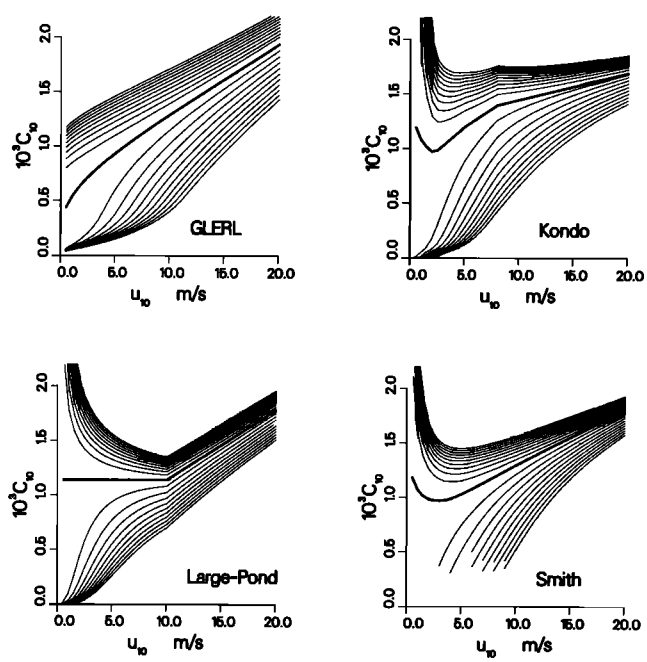

Fig. 2. Comparison of different bulk transfer coefficient formulas as a function of 10-m wind speed for air-sea temperature differences from −20°C to +20°C at 1°C increment. The heavy line is the neutral case.

3. DATA

There have been eight NOMAD buoys moored in the Great Lakes since 1981 in water depths ranging from 15 to 250 m (Figure 3). These buoys are boat shaped, 6 m in length, with an electronic payload for measuring wind speed, wind direction, barometric pressure, air temperature, sea surface temperature, and surface wave spectral data. Most of the meteorological sensors are located 5 m above the water surface. Data are reported hourly. The wind speed and direction, as well as air and surface water temperatures, are 8.5-min averages of samples obtained at 1-s intervals. The waves are measured with an accelerometer using an on-board Wave Data Analyzer system [*Steele and Johnson*, 1977] that transmits acceleration spectral data via the UHF GOES satellite to a shore collecting station, where wave frequency spectra with 48 degrees of freedom are calculated from 20 min of measurements. In this study we examined all the data recorded during 1981–1984, an average of over 4000 hourly measurements from each buoy every year. The results from different buoys and from

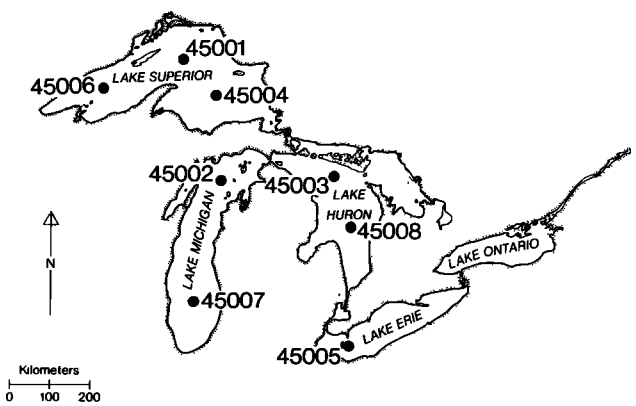

Fig. 3. Great Lakes map showing the locations of the eight National Data Buoy Center NOMAD buoys.

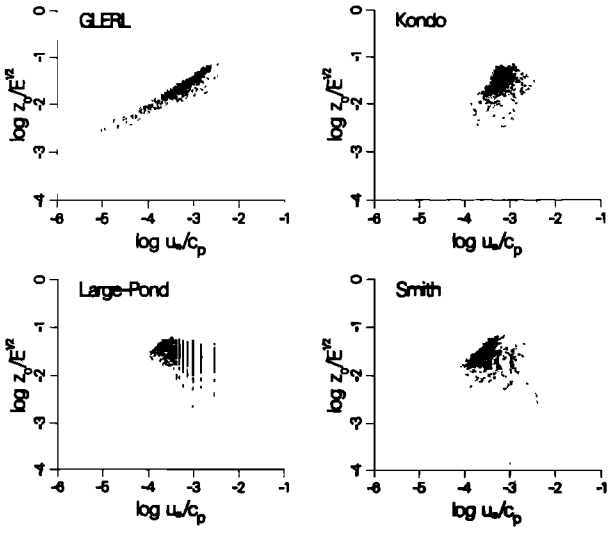

Fig. 4. Comparison of $z_0/E^{1/2}$ versus u_*/c_p correlations.

different years are very similar, however. Therefore the detailed analyses presented here use data from the 1984 northern Lake Michigan buoy number 45002 as representative of all the buoys. Buoy 45002 recorded 4212 simultaneous measurements of wind speed, air-sea temperature difference, significant wave height, and peak energy wave period in 1984 with a maximum wind speed of 15 ms^{-1} and a maximum significant wave height of 4.5 m. In the following analyses, calculations were based on all of the 4212 data points, while the graphs show only 1056 points (about every fourth point) in order to reduce crowding.

4. Results and Discussion

4.1. *Roughness Length*

The purpose of the empirical methods discussed above is to estimate values for the roughness length z_0 and for friction velocity u_* when these cannot be measured directly. The roughness length z_0 is conceptually an important parameter in the study of wind waves. However, it is difficult to measure or even define physically. Of the four methods we considered here, only the GLERL and Smith methods use z_0 explicitly; the Kondo and Large-Pond (as interpreted by *Keller et al.* [1985]) methods do not, although a value for z_0 can be estimated from these methods. To examine these z_0 estimations in connection with sea state studies, we follow *Huang et al.* [1986] and plot z_0 normalized by rms wave height $E^{1/2}$ versus u_* normalized by peak energy wave speed c_p. The results are shown in Figure 4. The GLERL method is the only one that shows a consistent correlation between normalized values of z_0 and u_*; this merely reflects the use of the Charnock relation in that method. The Smith method uses a nonlinear function for z_0 that approaches the Charnock relation at large u_*. The Kondo and Large-Pond methods do not use z_0 explicitly. None of these methods show any clear correlation between the normalized z_0 and u_*. Since all four methods are primarily formulated to estimate the drag coefficient C_z and the friction velocity u_* under diabatic conditions, z_0 did not receive a detailed treatment. The results of the correlations reflect this effect. The exact form of the relation between z_0 and u_* is still an active area of research; *Greenaert et al.* [1986], for example, discuss six different models for the relation.

4.2. *u_* Normalizations*

To examine the results for u_*, we apply the estimated u_* to the normalization of wind wave parameters. For a given wind and wave field with wave spectral energy density $S(f)$, total wave energy $E = \int S(f)\, df$, peak energy wave frequency f_m, and fetch distance F, the following parameters have been frequently used in the literature [e.g., *Hasselmann et al.*, 1973; *Mitsuyasu et al.*, 1980]: $\varepsilon_* = gE/u_*^2$, the nondimensional energy; $\nu_* = f_m u_*/g$, the nondimensional peak energy frequency; and $\xi_* = gF/u_*^2$, the nondimensional fetch. We affix a subscript z to the parameters which are normalized directly with measured wind speed u_z.

Correlating these various parameters has led to a number of universal power law relations that played important roles in developing numerical wave prediction models. *Hasselmann et al.* [1973, 1976], *Mitsuyasu et al.* [1980], and *Toba* [1978] have all deduced similar empirical equations characterizing the correlations among the parameters based on their own

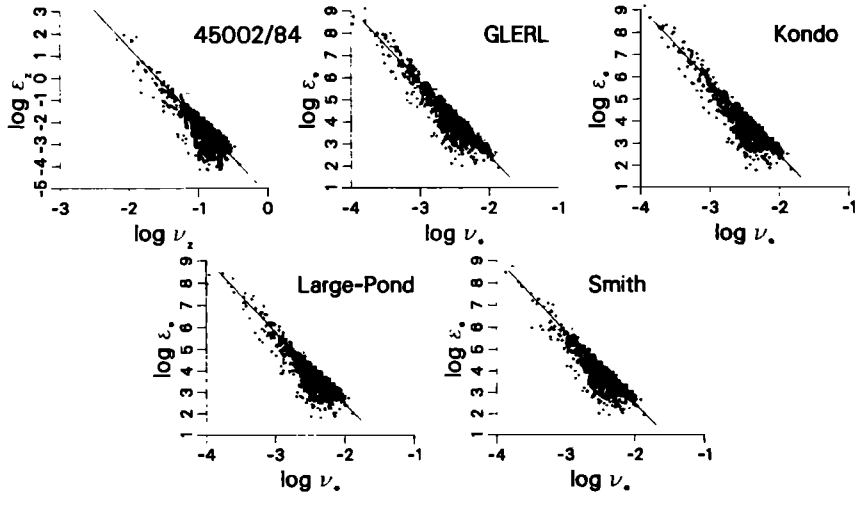

Fig. 5. Comparison of ε_* versus ν_* correlations. The straight lines are given by JONSWAP relations $\varepsilon = 5.3 \times 10^{-6}\nu^{-10/3}$ and $\varepsilon_* = 5.3 \times 10^{-5}\nu_*^{-10/3}$.

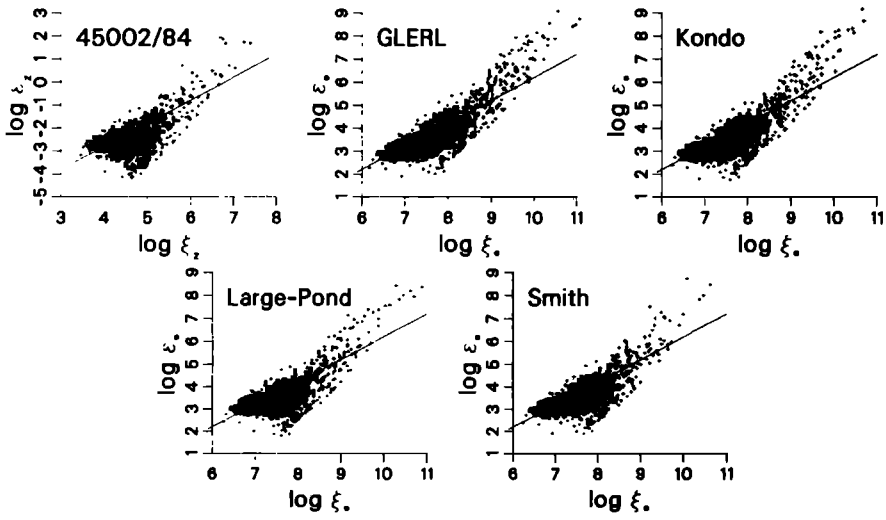

Fig. 6. Comparison of ε versus ξ correlations. The straight lines are given by JONSWAP relations $\varepsilon = 1.6 \times 10^{-7}\xi$ and $\varepsilon_* = 1.6 \times 10^{-4}\xi_*$.

measurements. An examination of these universal correlations was given by *Liu* [1984, 1985].

Figures 5–7 present the three intercorrelations ν versus ξ, ε versus ξ, and ε versus ν, respectively. In each figure we present the u_z normalization graph along with four u_* normalization graphs corresponding to the four methods. The empirical JONSWAP relations [*Hasselmann et al.*, 1973, 1976] for the respective parameters are plotted as the straight line in each graph for reference. As discussed by *Liu* [1985], the data points appear to be clustered around galaxylike regions rather than universal lines. The straight lines provide only a crude approximation of the data that can be accurate at times and erroneous at other times. This may be due to failure of the simple power law relations in unsteady conditions or to other processes. The power laws were developed mainly from growing sea states, whereas the data in Figures 5–7 represent both growing and dissipating waves. As shown by *Liu* [1985], however, even using carefully selected growth episodes does not lead to less scatter in the correlations. Clearly, none of the four methods of u_* estimation show any particular advantage in reducing the scatter. The scatter shown in the u_* normalization graphs is somewhat less than the u_z normalization graphs.

4.3. *Assessments*

In order to examine the correlations shown in Figures 5–7 on a quantitative basis we calculated and compared several statistical entities relevant to the correlations. Specifically, we sought the general relation $y = cx^b$ from our data and analyze the results statistically. Since all the correlations are plotted on the log-log scale, we simply let $X = \log(x)$, $Y = \log(y)$, and $a = \log(c)$, and by fitting a straight line of the form $Y = a + bX$ through the data points by least squares method we can calculate the following:

$$\text{standard error} = [\Sigma(Y - a - bX)^2/(n-2)]^{1/2} \quad (12)$$

$$\text{percentage deviation} = \Sigma|(Y - a - bX)/Y|(100/n) \quad (13)$$

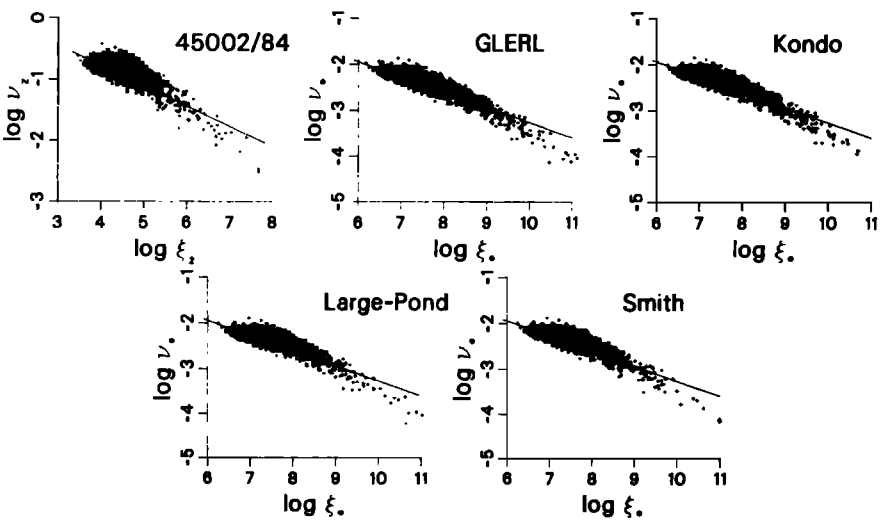

Fig. 7. Comparison of ν versus ξ correlations. The straight lines are given by JONSWAP relations $\nu = 3.5\xi^{-0.33}$ and $\nu_* = 1.08\xi_*^{-0.33}$.

TABLE 3. Summary of Calculated Standard Errors and Percentage Deviations for the Various Correlations

Nomalization	Standard Error			Percentage Deviation		
	ε versus v	ε versus ξ	v versus ξ	ε versus v	ε versus ξ	v versus ξ
u_z	0.384	0.578	0.133	17.24	30.27	11.98
GLERL u_*	0.373	0.581	0.135	6.78	11.83	4.49
Kondo u_*	0.393	0.629	0.140	7.81	13.53	4.71
Large-Pond u_*	0.408	0.655	0.141	8.44	14.08	4.73
Smith u_*	0.364	0.540	0.130	7.17	11.52	4.38

where n is the total number of data points (4212 for our 1984 North Lake Michigan buoy data set). Table 3 lists the calculated standard errors and percentage deviations for each of the 15 correlations shown in Figures 5–7. A well-fitted correlation should provide lower standard error and lower percentage deviation.

An examination of Table 3 shows that based on the calculated standard errors alone we are still unable to make any distinction among the various normalizations. For each of the three correlations, ε versus v, ε versus ξ, and v versus ξ, the standard errors are virtually the same. Since it is applied to $\log(x)$ and $\log(y)$, an average standard error of 0.4, as in the case of ε versus v, indicates that the actual estimates can vary by a factor of 2.5 from the regression line. Similarly, the average standard errors of 0.6 (ε versus ξ) and 0.135 (v versus ξ) lead to variation factors of 4.0 and 1.4, respectively.

When we examine the calculated percentage deviations, we find that there are significantly lower percentage deviations for the u_* normalizations. Among the four methods, although there are slight variations in the percentage deviations, none shows any particular advantage in improving the fit significantly. In general, either the GLERL, Kondo, Large-Pond, or Smith method can be used to provide u_* as well as u_{10} estimations for practical applications.

In the above analysis we predetermined the functional form of $y = ax^b$ and chose the dependent and independent variables y and x, respectively, according to the familiar JONSWAP formulations (that is, ε in terms of v, ε in terms of ξ, and v in terms of ξ). We also tried correlating them inversely by interchanging y with x as dependent variables as well as estimating the slope coefficient in the linear relationship by the maximum likelihood method [e.g., *Kendall and Stuart*, 1973]. While both of these analyses resulted in different sets of numbers, the implications are precisely identical to our previous discussions. Hence alternate analysis will not alter the results presented here.

In this analysis we have used all the data available without discriminating between cases representative of swell or wind waves. This is mainly because there is so little swell activity in Great Lakes waves that separation of swell cases from wind wave cases would not improve the results significantly.

In Figure 2 the GLERL method is considerably different from the other three methods at low wind speeds for unstable cases. Approximately 10% of the data we used in the analysis were of unstable cases with wind speed less than 5 ms^{-1}. However, we find there is no discernible difference due to this effect in the results. Apparently, this divergence does not have a significant effect on the parametric correlations.

5. Concluding Remarks

From detailed examination of the four methods used to estimate u_* from a given u_z and air-sea temperature difference and application of these estimates to wind-wave parametric correlations we expected to distinguish a method which effectively reduced the scatter. We find instead that the four methods examined are virtually indistinguishable. Because all methods follow the same basic approach, with different but comparable empirical formulations, this result is by no means surprising. In practice, any of the four methods will provide similar estimates of u_*. Until further detailed wind stress and wind profile measurements can be conducted to ascertain or validate the empirical formulations these methods will remain useful tools in providing wind stress, bulk transfer coefficients, and wind profile estimations where only minimal input data are available.

Acknowledgment. We would like to thank W. H. Brutsaert of Cornell University for initially suggesting this study. Great Lakes Environmental Research Laboratory contribution 509.

References

Businger, J. A., J. C. Wyngaard, Y. Izumi, and E. F. Bradley, Flux-profile relationships in the atmospheric surface layer, *J. Atmos. Sci.*, *28*, 181–189, 1971.

Charnock, K. H., Wind stress on a water surface, *Q. J. R. Meteorol. Soc.*, *81*, 639–640, 1955.

Dyer, A. J., A review of flux-profile relationships, *Boundary Layer Meteorol.*, *17*, 363–372, 1975.

Geernaert, G. L., K. B. Katsaros, and K. Richter, Variation of the drag coefficient and its dependence on sea state. *J. Geophys. Res.*, *91*(C6), 7667–7679, 1986.

Hasselmann, K., T. P. Barnett, E. Bouws, H. Carlson, D. E. Cartwright, K. Enke, J. A. Ewing, H. Gienapp, D. E. Hasselmann, P. Kruseman, A. Merrburg, P. Muller, D. J. Richter, W. Sell, and H. Walden, Measurements of wind-wave growth and swell decay during the Joint North Sea Wave Project (JONSWAP), *Dtsche. Hydrogr. Z.*, *A12*, 95 pp., 1973.

Hasselmann, K., D. B. Ross, P. Muller, and W. Sell, A parametric wave prediction model, *J. Phys. Oceanogr.*, 6, 200–228, 1976.

Huang, N. E., L. F. Bliven, S. R. Long, and P. S. DeLeonibus, A study of the relationship among wind speed, sea state, and the drag coefficient for a developing wave field, *J. Geophys. Res.*, *91*(C6), 7733–7742, 1986.

Keller, W. C., W. J. Plant, and D. E. Weissman, The dependence of X band microwave sea return on atmospheric stability and sea state, *J. Geophys. Res.*, *90*(C1), 1019–1029, 1985.

Kendall, M. G., and A. Stuart, *The Advanced Theory of Statistics*, vol. 2, chapter 29, Hafner Press, New York, 1973.

Kondo, J., Air-sea bulk transfer coefficients in diabatic conditions, *Boundary Layer Meteorol.*, *9*, 91–112, 1975.

Large, W. G., and S. Pond, Open ocean momentum flux measure-

ments in moderate to strong winds, *J. Phys. Oceanogr.*, *11*, 324–336, 1981.

Large, W. G., and S. Pond, Sensible and latent heat flux measurements over the ocean, *J. Phys. Oceanogr.*, *12*, 464–482, 1982.

Liu, P. C., In search of universal parametric correlations for wind waves, in *The Ocean Surfaces.*, edited by Y. Toba and H. Mitsuyasu, pp. 171–178, D. Reidel, Hingham, Mass., 1984.

Liu, P. C., Testing parametric correlations for wind waves in the Great Lakes, *J. Great Lakes Res.*, *11*, 478–491, 1985.

Long, P. E., Jr., and W. A. Shaffer, Some physical and numerical aspects of boundary layer modeling, *NOAA Tech. Memo. NWS TDL-56 (COM75-10980)*, 37 pp., 1975.

Mitsuyasu, H., F. Tasai, T. Suhara, S. Mizuno, M. Ohkusu, T. Honda, and K. Rikiishi, Observation of the power spectrum of ocean waves using a cloverleaf buoy, *J. Phys. Oceanogr.*, *10*, 286–296, 1980.

Monin, A. S., and A. M. Obukhov, Basic laws of turbulent mixing in the atmosphere near the ground, *Tr. Akad. Nauk SSSR Geofiz. Inst.*, *24*, 163–187, 1954.

Paulson, C. A., The mathematical representation of wind speed and temperature profiles in the unstable atmospheric surface layer, *J. Appl. Meteorol.*, *9*, 857–861, 1970.

Schwab, D. J., Simulation and forecasting of Lake Erie storm surges, *Mon. Weather Rev.*, *106*, 1476–1487, 1978.

Smith, S. D., Coefficients for sea-surface wind stress and heat exchange, *Report BI-R-81-19*, 31 pp., Bedford Inst. of Oceanogr., Bedford, Nova Scotia, Can., 1981.

Smith, S. D., and E. G. Banke, Variation of the sea surface drag coefficient with wind speed, *Q. J. R. Meteorol. Soc.*, *101*, 665–673, 1975.

Steele, K., and A. Johnson, Jr., Data buoy wave measurements, in *Ocean Wave Climate*, edited by M. D. Earle and A. Malahoff, pp. 301–316, Plenum, New York, 1977.

Toba, Y., Stochastic form of the growth of wind waves in a single-parameter representation with physical implications, *J. Phys. Oceanogr.*, *8*, 494–507, 1978.

P. C. Liu and D. J. Schwab, Great Lakes Environmental Research Laboratory, NOAA, 2205 Commonwealth Boulevard, Ann Arbor, MI 48105.

(Received September 5, 1986;
accepted February 5, 1987.)